Medical Engineering and Physics 69 (2019) 123–133

Contents lists available at ScienceDirect

Medical Engineering and Physics

journal homepage: www.elsevier.com/locate/medengphy

Numerical study of patient-specific ankle-foot orthoses for drop foot patients using shape memory alloy

Farshid Sadeghian, Mohammad Reza Zakerzadeh, Morad Karimpour*, Mostafa Baghani

School of Mechanical Engineering, College of Engineering, University of Tehran, P.O.B. 11155-4563, Tehran, Iran

ARTICLE INFO

Article history:
Received 2 January 2018
Revised 29 January 2019
Accepted 20 April 2019

Keywords:
Ankle-foot orthosis (AFO)
Shape memory alloy (SMA)
Drop foot
Stiffness
Pretibial weakness
OpenSim
Gait cycle

ABSTRACT

Drop foot is a nerve-muscle disorder that affects the muscles that lift the foot. The two main side effects of drop foot are slapping/kicking the foot after heel strike (foot) and dragging the foot during the swing (toe drag). Treatment methods such as ankle-foot orthoses (AFO) have some biomechanical benefits, but are not applicable to all walking conditions and cannot mitigate significant gait complications. This study introduces the design of a passive AFO system, which combines an ordinary AFO and a shape memory alloy (SMA) element. OpenSim was used to simulate patients with muscle weakness and to calculate the torque needed to imitate normal ankle joint stiffness. The calculated torque was then reproduced for different levels of muscle weakness by the superelasticity of SMAs. The study showed that the normal joint stiffness profile for each patient with a certain level of muscle weakness can be restored by designing a patient-specific orthosis.

1. Introduction

Walking is crucial for human mobility; however, millions of people have impaired gait as a result of neuromuscular disorders [1]. Ankle dorsiflexor muscles play an important role throughout the gait cycle. Drop foot is a motor deficiency caused by general or relative paralysis of the muscles innervated by the common peroneal nerve or paralysis of the anterior tibial muscle and the peroneal group [2]. Major complications of drop foot during walking include: (1) slapping the forefoot after heel strike, and (2) pulling the toes at the beginning of each swing phase. In a patient with drop foot, hitting the heel is followed by the foot moving uncontrollably towards the ground and producing an abnormality (foot slap) [3]. Toe drag prevents proper limb advancement and increases the risk of tripping during the mid-swing phase of the gait cycle. As a result, patients suffering from drop foot disorder either scuff their toes on the ground, or bend their knees to raise their feet higher than usual to prevent scuffing, causing a “steppage” gait. Drop foot forces the patient to move the hip joint extensively during the swing phase to prevent their toes contacting the ground and to ensure they reach the ground with the forefoot [4]. These patients tend to walk with difficulty and suffer from fatigue, which affects their walking speed and distance. Drop foot is an indication of a major problem and, depending on the cause, can be temporary or permanent.

Causes of drop foot include neurodegenerative disorders of the brain that lead to muscular problems, such as stroke and cerebral palsy; motorneuronal disorders, such as polio; some forms of muscular spasm atrophy; amyotrophic lateral sclerosis; damage to the nerve root, such as stenosis; and spinal cord and peripheral neurological disorders [3].

Immobilization and not using the affected joints can worsen the outcome. Staying in a fixed position for a long time can lead to muscle shortening and worsening of contractions and spastic reflexes [5,6]. One of the most common treatments for drop foot is ankle-foot orthoses (AFOs) [7]. In 2002, a statistical study by Nielson showed that more than 2 million people in North America are partially or completely paralyzed, and that 20.3% of these people utilize orthoses to improve their gait pattern [8]. AFOs are designed to protect and align the ankle and foot to mitigate contraction force on the associated muscles, help the weak or paralyzed muscles of the ankle and foot, and prevent and modify the deformities [9]. Orthotic devices can be used to stretch the affected muscles to return them to their physiological posture and increase the range of movement of the joints.

Kobayashi et al. designed and fabricated an ankle orthosis with springs and adjustable mechanical properties. The orthosis was tested on post-stroke patients and motion analysis showed that a change in orthosis properties led to changes in the kinetics and kinematics of the knee and ankle joints [10]. Bhadane et al.

* Corresponding author.
E-mail address: m.karimpour@ut.ac.ir (M. Karimpour).

https://doi.org/10.1016/j.medengphy.2019.04.004
1350-4533/

designed an ankle-knee brace using a shape memory alloy (SMA) wire to mimic the stiffness profile in a normal ankle [11]. By laying SMA wires in regular braces, they designed a brace for patients with normal ankle plantar flexion but difficulty in dorsiflexion motion. Bhadane showed that the placement of two parallel SMA wires was very useful for mimicking healthy ankle stiffness characteristics and states. Deberg et al. provided an actuator made of Nitinol superelastic alloys that had faster reaction times and made the brace more practical and effective for walking [12,13]. Plantar flexion of the ankle pushes the SMA wires and prevents excessive ankle plantar flexion, and stores energy to help dorsiflexion. Results of motion analysis indicated that the brace can help the abnormal gait cycle in drop foot patients. As suggested by Andani et al., a brace consisting of a superelastic SMA rod as a passive actuator is based on a multi-axial loaded rod that is parallel to the ankle axis. It was exposed to torsional load due to the rotation of the ankle and the rotational load, and the linear motion of the solenoid actuator. The multi-axial load enables adjustment of the rod rotational stiffness during the gait cycle and creates different levels of stiffness at different speeds [14]. Another design was proposed by Mataee et al. for a superelastic SMA actuator under bending torques consisting of superelastic hinges, an adjustable joint, a linear actuator and a slider. In this model, the linear actuator determines the position of the slider and adjusts the hinge length, which results in the distinct stiffness required in the ankle [15]. Another study by Pittaccio et al. showed that the superelastic Nitinol alloy can be used with a specific shape in the actuator springs and this holds the ankle in a steady state and reduces spasm around the ankle [16]. In another study, Facchinello et al. assessed the use of monolithic superelastic rods with variable flexural stiffness for spinal fusion: they concluded that such alloys could be utilized to define an optimum stiffness profile for implants [17].

These orthoses improve gait by reproducing the overall stiffness of the healthy joint. The weak muscle of the patient can produce some portion of the torque required. The activity and power of healthy muscles reduce after all the torques needed during the gait cycle have been generated. By producing all the torque needed for the joint during the gait cycle, it is not possible to achieve the stiffness of a normal joint. This type of design reduces the healthy muscle input and produces more torque, which results in more pressure on the plantar flexion ankle in passive orthoses. The needs of each patient are assessed individually using motion analysis [18] and the required torque is reproduced to achieve the stiffness of a normal joint.

The aim of this study was to design an ankle orthosis to provide normal ankle movement in patients with dorsiflexor muscle weakness. The torque needed to correct patient kinematics can be achieved through placing an actuator at the ankle joint and using motion analysis and simulation of the patient in OpenSim software. Therefore, this method enables analysis and design of orthosis for patients with different degrees of muscle weakness. Inserting the SMA element in a regular brace reproduces the stiffness of a healthy ankle joint and a more natural gait pattern is achieved. The SMA element is employed to reproduce the required stiffness using the Finite Element Method (FEM) in ABAQUS software and the user's sub-routines written for an SMA based on the Brinson constitutive equations [19].

2. Ankle behavior

The basic features of the normal gait pattern in the patient are identified by studying the kinematics and kinetics of a healthy ankle during the gait cycle. In normal walking when loading the limb, the ankle-plantar flexion torque leads to the foot movement towards the ground. Ankle motion provides propulsion to the leg during the mid-stance phase. A dorsiflexion torque is provided by the movement of the body over the foot, when the foot is still in contact with the ground. At heel-off, the reactive force of the ground is transmitted to the front of the foot. This results in more dorsiflexion torque during the terminal stance. At the end of terminal stance, the plantar flexes of the legs occur in response to the calf muscle movement - this is called push-off. The pretibial muscles cause foot dorsiflexion in the beginning of the swing phase. The dorsiflexion torque decreases in the mid-swing phase. Finally, the ankle position will be controlled again by pretibial muscles at the end of the swing to match the requirements of the force, which is desirable for the next initial contact [20,21].

Table 1
Four-step loading-unloading rotation of the ankle [15].

Step	Phase	Rotation [°]	State
1	Loading response	6.5	Loading
2	Mid- and terminal stance	17	Unloading
3	Pre-swing	27	Loading
4	Swing	16.5	Unloading

The stiffness of the ankle joint is considered to be the resistance to ankle rotation during walking [22]. This stiffness includes intrinsic stiffness and reflex stiffness. Intrinsic stiffness is related to muscular structures of the joint, whereas reflex stiffness is related to muscular function in the flex and reflex action [23–25]. Ankle joint stiffness is achieved through a combination of joint angles and the generated torque during walking in normal conditions. A study by Bhadane-Deshpande used motion analysis to investigate healthy foot and drop foot at various speeds [11]. Fig. 1 shows the angular changes for a healthy foot and an affected foot in a patient with pretibial weakness. Although the stiffness of the ankle is non-linear (see Fig. 1), the division of the entire gait into separate events forms four linear stiffness curves. Additionally, these four events can simply be modeled with two loaded and unloaded modes.

The main movements of the ankle joint occur during walking on a sagittal surface (normal level of movement of the body). Therefore, the kinematics of a healthy and abnormal ankle at the sagittal level are examined [26]. A four-step behavior is observed with classification of the entire motion gaits into loading and unloading events. Table 1 includes a four-step rotation of the ankle input from the experimental data [11,27,28]. For a person of 70 kg with a specific gait length of 1.25 s (which is close to normal conditions), this gait consists of 6.5° of rotation in plantar flexion that is loaded onto the ankle during the loading process. Therefore, 17° of rotation occurs in dorsiflexion during the mid- and end-state. In the pre-swing stage, the ankle plantar flexes have 27° of rotation. At the end, at swing, the entire rotation is retrieved with a 16.5° dorsiflexion. A simplified dual loading-unloading phase is used to perform simulation that includes 16.5° rotation in steady state and 16.5° retrieval during swing [15].

To identify ankle deficiency, gait analysis was performed by Bhadane-Deshpande on a drop foot patient walking without any AFO [11]. The stiffness of the affected joint is depicted by a dashed line in Fig. 1. Patients with drop foot cannot control the foot segment and are unable to raise the foot in the swing phase. As shown in the figure, while patients are walking with the affected leg without AFO, the angle remains in plantar flexion and does not return to dorsiflexion for the next impact. Compared with the change in angle of a healthy ankle, there was a major deficiency in the initial state, which is defined as the slap foot. Controlled plantar flexion is required to avoid this problem. Similarly, as shown in Fig. 2, the toe drag means a deficiency in the mid and end phases of the swing, which requires lifting the entire foot segment. Position (a) is depicted for the proper foot and (b) for the drop foot.

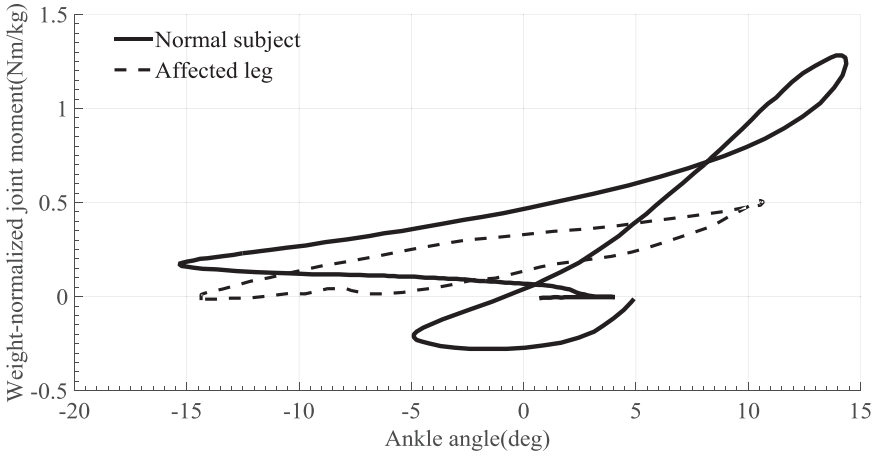

Fig. 1. Stiffness of healthy joint versus stiffness of weakness of pretibial muscles [11].

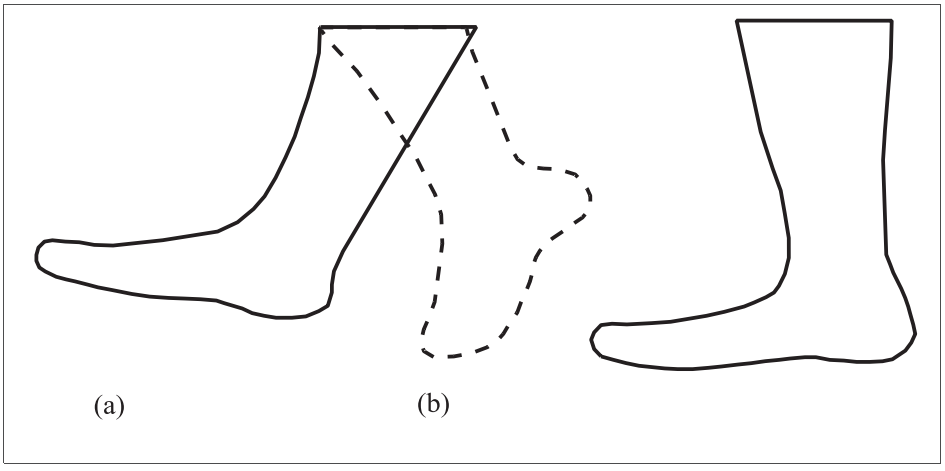

Fig. 2. Drop foot disability during walking: (a) normal foot and (b) drop foot.

To establish the stiffness requirements that must be achieved by the SMA element, the stiffness characteristics of the healthy leg are compared with those of the affected leg of the patient with drop foot. Furthermore, age clearly affects muscle stiffness, so this is also taken into consideration. Early stance and mid-swing phases require increased stiffness. Primary stiffness can be obtained by a passive spring and only provides resistance to plantar flexion. However, stiffness modulation is required in the swing phase, so we decided to focus on SMA simulation in the swing phase to help drop foot patients to raise their foot towards dorsiflexion.

3. Shape memory alloy (SMA) behavior

Identifying the behavior of the SMA and its loading response with respect to the ankle joint is essential in designing the orthotic device. The SMA has been used recently in a wide range of medical and aerospace engineering equipment, including cardiovascular stents, orthodontic arches and cellular phone antennae, because of its good fit with the human body, low weight and low volume, and non-linear mechanical properties [29]. This class of materials shows two distinct behaviors: shape memory effect (SME) characteristics in low temperatures and superelastic characteristics in high temperatures. These behaviors relate to the change of solid state phase between austenitic and martensitic crystal profiles [30]. The change in this phase is due to a thermo-mechanical phenomenon caused by changes in temperature or stress. Superelasticity or pseudo-elasticity receive considerable pressure through mechanical loading and unloading, without any change in the SMA temperature. This behavior is observed when the loading and unloading occur at a temperature higher than the austenitic temperature without stress (i.e. A_f). The thermo-mechanical loading path begins at a high temperature above A_f, so the austenitic phase does not change. Therefore, as a result of applying the force on the alloy, the detwinned martensitic phase will be formed, which dissolves after the load loss [34]. Nitinol SMA has many applications with unique elastic characteristics that lead to large deformations during loading and unloading.

4. The proposed orthosis mechanism

The aim of orthosis is to modify the walking pattern of the patient. The proposed orthosis consists of an SMA element that helps to save energy during plantar flexion and releases it during dorsiflexion to the ankle joint based on the concept proposed in this paper. Placing the SMA element parallel to the joint means the SMA is under the same ankle rotation; therefore, the ankle rotation is regarded as an input for the main loading conditions.

In this study we developed a series of hinges that can be used to create compatible orthoses to accomplish these concepts. Two elements made of NiTi are placed inside the hinges in the form of a large Omega (i.e. Ω). This special form causes the material to be loaded all the way, avoiding the focus of the stresses and finally failure. SMA performance is based on pseudo-elasticity. Non-linear and hysteresis behavior of NiTi SMA brings convenient properties

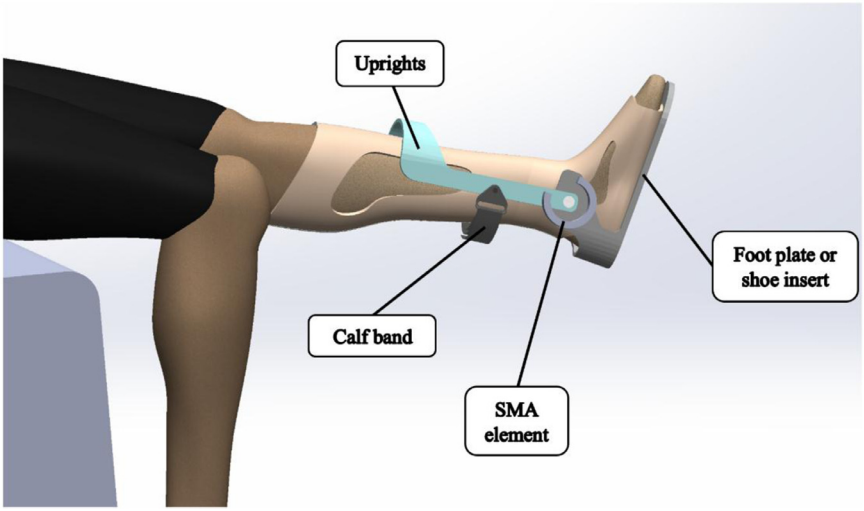

Fig. 3. The Proposed design for the hinge ankle orthosis.

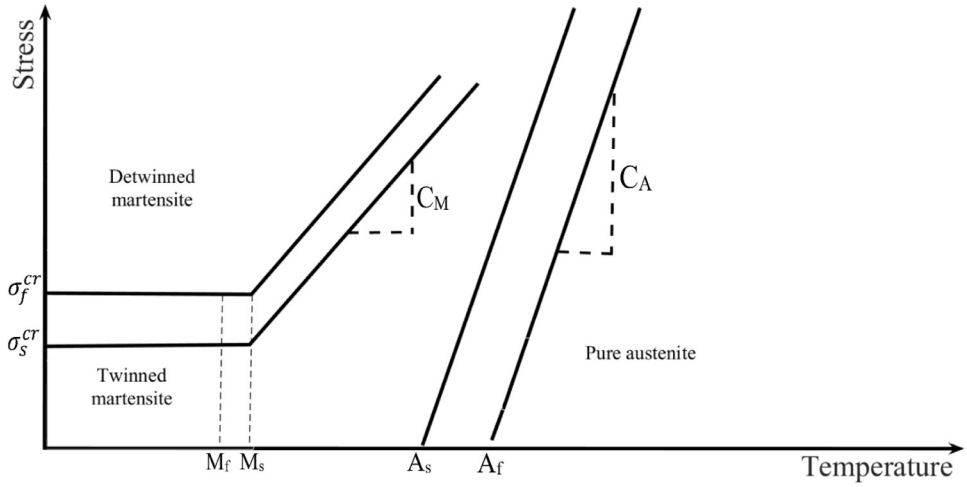

Fig. 4. Critical stress-temperature profiles used in the Brinson model [32].

to the proposed orthoses in this application, and removes the problems related to dynamic splints with fully elastic elements. A change in elongation in components with elastic characteristics leads to a change in spring-back forces; preloading these components so they reposition to the desired posture means the corrective force applied to the limb will be large at the beginning of the process and will gradually decrease as close as possible to the joint angle and target. Clockwork torsional springs can be employed to respond to this effect, but they can be weak or bulky. In contrast, the non-linear behavior of pseudo-elastic SMA, due to a long plateau in a quasi-constant pressure, enables continuous therapeutic action even in the vicinity of the target and for a greater range of deformations/stretches.

By choosing appropriate thermo-mechanical treatments for the shape-setting step, different SMA elements with varying length and pressure (deformation) can be used and the properties of the alloy can be adjusted for the different needs of the patient. Thus, the following can be achieved simultaneously: (1) providing a corrective biomedical, biometric, and clinical pressure, which the patients may be able to tolerate; (2) maximizing acceptability of the recommended treatment with sufficient corrective pressure and matching orthosis with involuntary shocks, which reduce the pain caused by lengthening the spastic muscles; 3) avoiding limb stability, and thus improving joint mobility and the possibility of using the rest of the limb; 4) removing the need to regulate the spring preload as a position to improve the worker's status and work load; and 5) articulate auto-tuning the movement direction; the stress during loading is greater than the time of discharge by the SMA hysteresis. Therefore, conventional spring stiffness is greater for actions that are unlike clinical goals. One of the important advantages of pseudo-elastic devices, such as SMAs, over conventional devices is that conventional orthoses tend to increase viscoelastic stiffness during treatment due to immobility and non-use of damaged joints, whereas pseudo-elastic orthoses dissolve the viscoelastic stiffness over the same time period. The proposed orthosis comprises three main parts: tibial upright, foot plate and SMA element. As shown in Fig. 3, the tibial upright and foot plate are attached to each other with a conventional hinge joint, and an SMA element is employed parallel to the ankle joint; the proposed orthosis is attached to the calf of the patient with a calf band.

5. Numerical model for SMA element of the proposed orthosis

Numerous methods have been proposed for modeling SMA behavior. The Finite Element Method (FEM) is one of the most common numerical methods and has been used in many studies. In this paper, the non-linear behavior of SMA is simulated using the

Table 2
Material parameters adopted for the Tokuda et al. (1999) experiment [33].

Property	Unit	value
Moduli	GPa	$D_m^+ = 26,\ D_m^- = 33,\ D_a = 34.9,\ D_m^T = 26$
Transformation stresses	MPa	$\sigma_s^+ = 70,\ \sigma_f^+ = 188,\ \sigma_s^- = 0,\ \sigma_f^- = 220$
Stress-temperature slopes	MPa/ °C	$C_M^+ = 1,\ C_A^+ = 3,\ C_M^- = 0.2,\ C_A^- = 3$
Transformation strain	–	$\varepsilon_L^+ = 0.016,\ \varepsilon_L^- = -0.0146$
Thermo-elastic modulus	MPa/ °C	$\theta = 0.55$
Transformation temperatures	°C	$M_f = -55,\ M_s = -35,\ A_s = -30,\ A_f = -15$

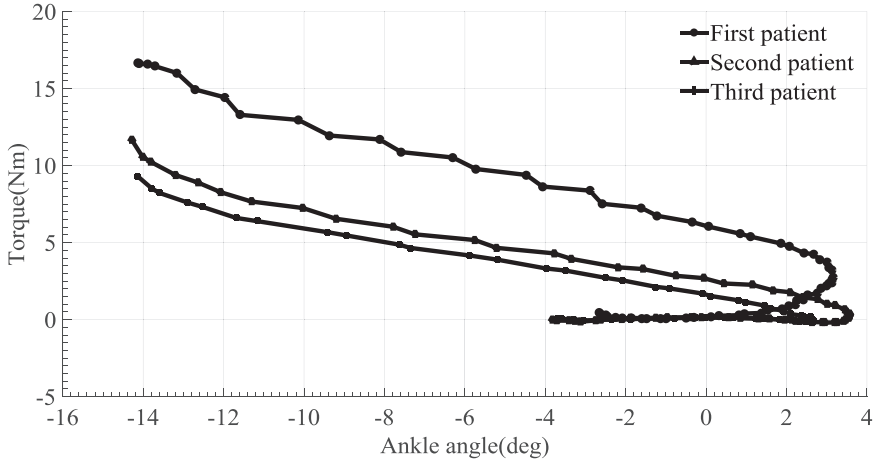

Fig. 5. Appropriate actuator (simulation in OpenSim) stiffness to improve gait pattern for different patients.

subset of the user generated by the Brinson constitutive equations by the FEM in ABAQUS [19]. This model is described briefly below.

In the Brinson and Huang model, separating the martensite volume (ξ) into temperature-induced martensitic (ξ_T) and stress-induced martensitic (ξ_S), the Liang and Roger transformation equation with critical stress is used to identify ξ_S and ξ_T to the SME at low temperature M_s [31]. The critical temperature-stress profile used in the Brinson model is shown in Fig. 4.

The martensite volume fraction (ξ) separation can be considered as the following [32]:

$$\xi = \xi_S + \xi_T \tag{1}$$

The constitutive equation for stress (σ), strain (ε) and temperature (T) in the form of martensitic volume fraction (ξ) is as follows:

$$\sigma = E(\xi)(\varepsilon - \varepsilon_L \xi_S) + \Theta(T - T_0) \tag{2}$$

here ε_L is the maximum strain that can be retrieved [32]. E stands for the elastic modulus and is regarded as a linear function of the martensitic volume fraction [31]:

$$E(\xi) = E_A + \xi(E_M - E_A) \tag{3}$$

where E_M and E_A stand for the elastic modulus in martensite and austenite phases, respectively. At zero stress point, phase transformation is triggered at desired temperatures by M_s, M_f, A_s, and A_f, which denote the martensite start, martensite finish, austenite start, and austenite finish temperatures, respectively. The stresses of detwinning start and finish process are as σ_s^{cr} and σ_f^{cr}, respectively. C_M and C_A (see Fig. 4) are constants that show the influence-stress coefficients, and indicate the stress effect on transformation temperature of the martensite and austenite phases, respectively [31].

The evolution of equations for calculating martensitic fractions as a function of temperature and stress, as shown in Fig. 4, can be specified as follows:

For $T > M_S$ and $\sigma_s^{cr} + C_M(T - M_S) < \sigma < \sigma_f^{cr} + C_M(T - M_S)$

$$\xi_S = \frac{1 - \xi_{S0}}{2} \cos\left\{\frac{\pi}{\sigma_S^{cr} - \sigma_f^{cr}}\left[\sigma - \sigma_f^{cr} - C_M(T - M_S)\right]\right\} + \frac{1 + \xi_{S0}}{2}$$

$$\xi_T = \xi_{T0} - \frac{\xi_{T0}}{1 - \xi_{S0}}(\xi_S - \xi_{S0}) \tag{4}$$

Also, for $T < M_S$ and $\sigma_s^{cr} < \sigma < \sigma_f^{cr}$

$$\xi_S = \frac{1 - \xi_{S0}}{2} \cos\left\{\frac{\pi}{\sigma_S^{cr} - \sigma_f^{cr}}\left(\sigma - \sigma_f^{cr}\right)\right\} + \frac{1 + \xi_{S0}}{2}$$

$$\xi_T = \xi_{T0} - \frac{\xi_{T0}}{1 - \xi_{S0}}(\xi_S - \xi_{S0}) + \Delta_{T\varepsilon} \tag{5}$$

where, if $M_f < T < M_S$ and $T < T_0$

$$\Delta_{T\varepsilon} = \frac{1 - \xi_{T0}}{2}\left\{\cos\left[a_M\left(T - M_f\right)\right] + 1\right\}$$

else $\Delta_{T\varepsilon} = 0$ (6)

For $T > A_S$ and $C_A\left(T - A_f\right) < \sigma < C_A(T - A_S)$

$$\xi = \frac{\xi_0}{2}\left\{\cos\left[a_A\left(T - A_S - \frac{\sigma}{C_A}\right)\right] + 1\right\}$$

$$\xi_s = \xi_{s0} - \frac{\xi_{s0}}{\xi_0}(\xi_0 - \xi)$$

$$\xi_T = \xi_{T0} - \frac{\xi_{T0}}{\xi_0}(\xi_0 - \xi) \tag{7}$$

where $(T_0, \xi_{S0}, \xi_{T0}, \xi_0)$ represent the material initial state. Also, a_A and a_M are the constants of material as follows:

$$a_A = \frac{\pi}{A_f - A_s} \tag{8}$$

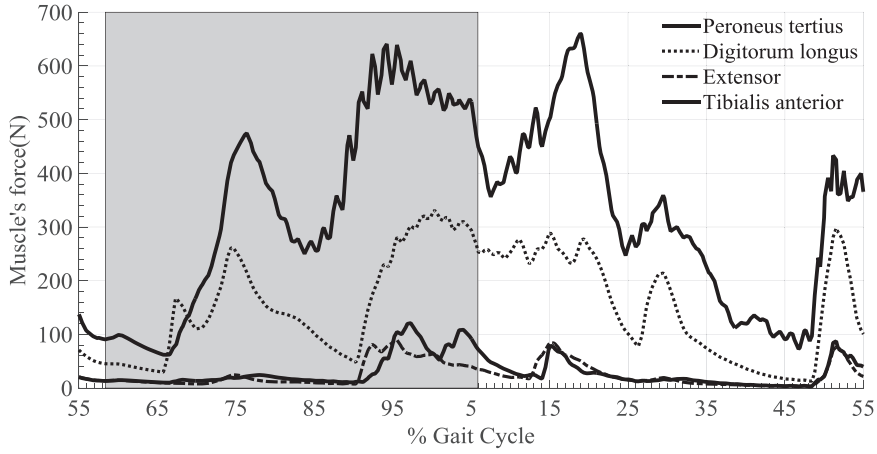

Fig. 6. Dorsiflexor muscles activity for a normal gait cycle.

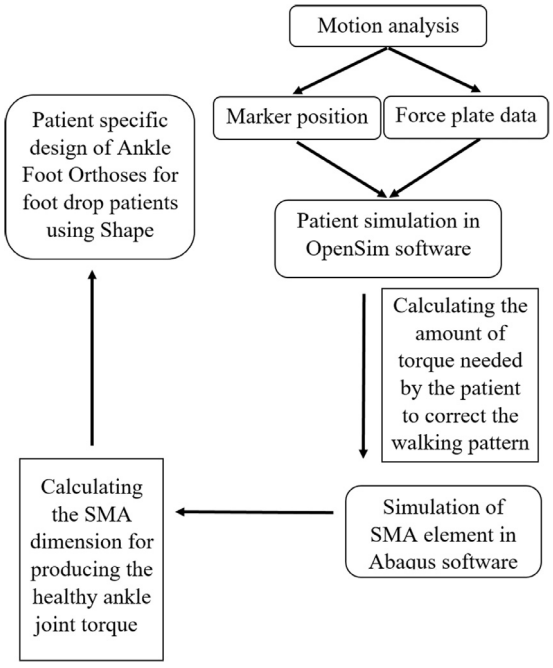

Fig. 7. The algorithm used for designing the proposed patient-specific AFO for drop foot patients.

$$a_M = \frac{\pi}{M_s - M_f} \tag{9}$$

SMA behavior is determined using the non-linear function of stress, pressure and temperature, which are not correlated with each other. The SMA beam parameters were derived using results from tests conducted by Tokuda et al. [33]. Positive and negative model parameters denote them under tension and compression loading, respectively. Notably, the temperature A_f for this alloy is −15 °C, which enables the daily use of orthosis at ambient temperature as the alloy shows superelastic properties. The SMA material parameters are listed in Table 2.

6. OpenSim software

The degree of pretibial muscle weakness varies between patients; therefore, it is not possible to improve the gait patterns of all patients using only one orthosis. In this study, appropriate orthoses were designed using specific motion analysis data from each patient to reproduce a healthy joint stiffness for each individual. The experimental data in this study include gait analysis data, electromyography (EMG) and anthropometric data of the patient. Six dynamic and three static tests were performed during data collection. The runtime of each dynamic test was about 5 s and consisted of 5 steps; the runtime of each static test was about 10 s. A total of 43 markers were used at each time step to determine the angles of the joint in the motion analysis test.

Muscular activities can be achieved during the gait cycle using motion analysis and the patient modeling test in OpenSim. The level of muscle weakness can be determined by comparing these data with normal muscle activity. By inserting an actuator at the ankle joint of the patient, combining muscle weakness in the model and using the normal gait pattern kinematics in OpenSim, the torque needed to achieve the required kinematics is calculated using the Calculated Muscle Control (CMC) algorithm. The amount of torque required by the actuator in OpenSim should be equal to the torque difference created between the patient and the healthy individuals with the same kinematic condition. The CMC algorithm calculates the amount of muscle excitation during the gait cycle due to the kinematics of a patient. This algorithm calculates the force distribution between muscles at each stage by a static optimization criterion and a proportional derivative (PD) controller, so a forward dynamic simulation is created that follows the kinetics of the patient. When the patient suffers from muscle weakness, their muscles cannot produce enough power to reach the kinematics of a healthy person. The optimum torque required to produce the kinematics in the forward process can be calculated by inserting an actuator at the ankle joint at any time according to the anatomy and muscle co-operation. The actuator generates the required torque at any given time to reach optimal kinematics [34].

As the level of muscle weakness varies among patients, the torque curve created with the actuator is also expected to vary for different patients during the gait cycle. Therefore, the torque required for each patient should be individually calculated to correct their kinematics. The torque required for the joint and the swing middle and final phases is generated using the superelastic SMA beam bending stiffness. In this paper, a process is used for three groups of patients with varying degrees of muscle weakness. To reproduce the stiffness of a healthy joint and obtain the desired kinematic, the SMA element should produce the dorsiflexion torque in the swing and the initial contact phases, which is created by the actuator in OpenSim. Dorsiflexor muscles in the ankle joint include four muscles: tibialis anterior, extensor, digitorum longus and peroneus tertius. Patients with various levels

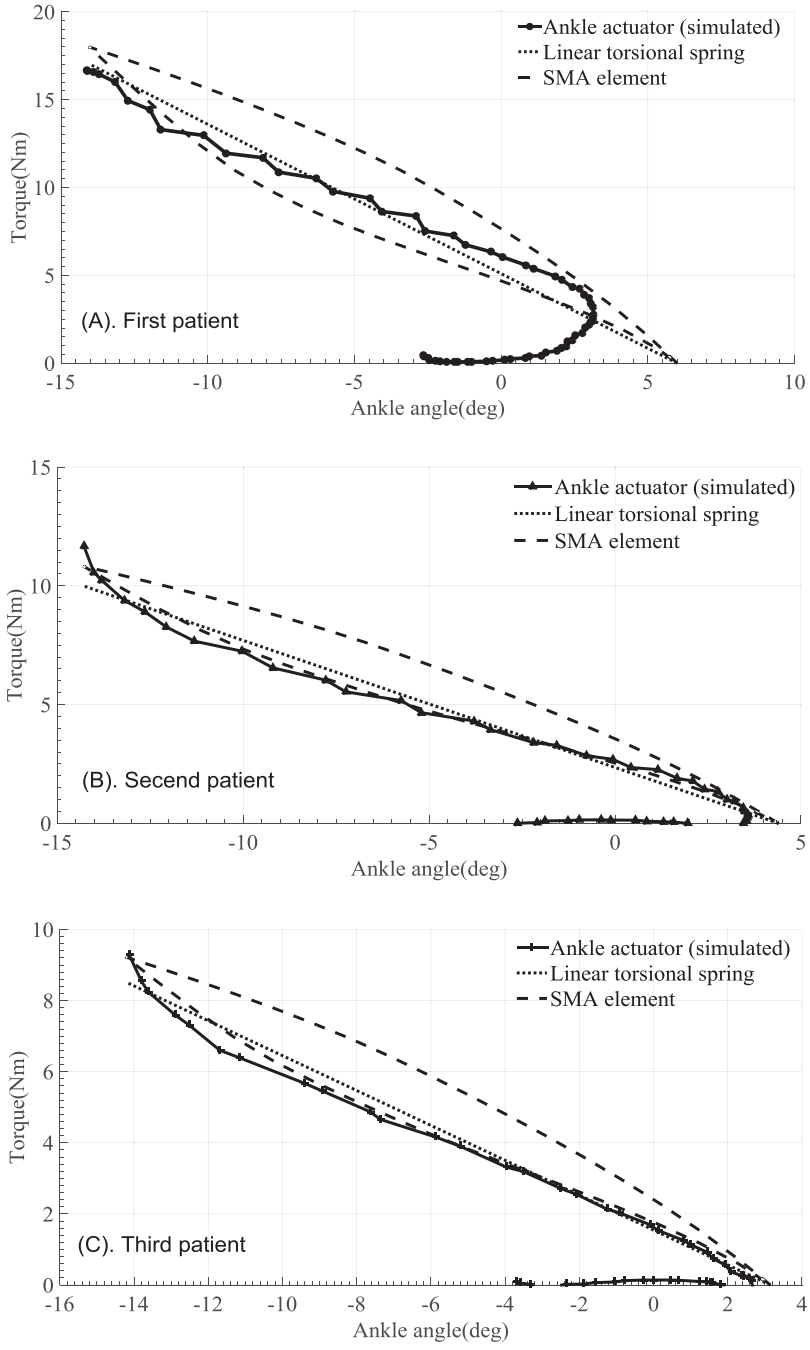

Fig. 8. Appropriate SMA elements and linear torsional spring designed to reproduce the stiffness of the actuator (simulation in OpenSim) for different patients.

Table 3
Characteristic of patients with different levels of pretibial muscle weakness.

	Tibialis anterior	Extensor	Digitorum longus	Peroneus tertius
First patient	–	–	–	–
Second patient	–	+	+	–
Third patient	–	+	+	+

of pretibial weakness have disability and weakness in one or more of these muscles. Three patients with weaknesses in at least one of these muscles were chosen for analysis, see Table 3.

In this paper, an orthosis with a superelastic SMA element was designed for the three patients with different degrees of weakness in the pretibial muscles (see Table 3). The first patient had lost all the ankle dorsiflexor muscles in OpenSim. Hence, the generation of all torque required for ankle dorsiflexion motion is inevitable for patients with pretibial muscle weakness. The second patient had weak tibialis anterior and peroneus tertius muscles; as the digitorum longus and extensor muscles of the second patient were healthy, a torque less than that for the first patient was needed to correct the gait pattern. The third patient had only a weak tibialis anterior muscle; as the ankle dorsiflexion muscles were healthy, a

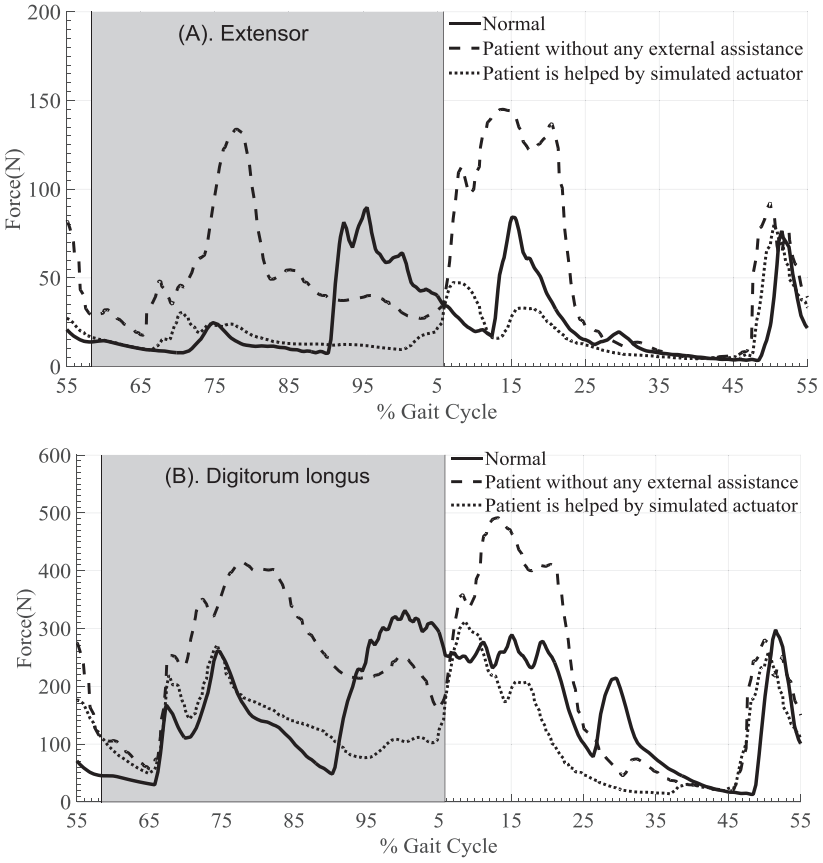

Fig. 9. The gait cycle for three cases: a healthy subject, the second patient with muscle weakness, and when using the actuator.

Table 4
Characteristics of scenarios with similar levels of pretibial muscles weakness to the first patient.

Scenarios	Tibialis anterior	Extensor	Digitorum longus	Peroneus tertius
First scenario	–	–	–	+
Second scenario	–	+	–	–
Third scenario	–	+	–	+

lower torque was expected to be needed to modify the gait pattern compared with for the first and second patients. Fig. 5 shows that different levels of torque, achieved by manipulating the actuator on the ankle joint in OpenSim software, were needed to reproduce the stiffness of the ankle joint for patients with different levels of muscle weakness.

Patients with drop foot do not have normal gait patterns because they cannot create dorsiflexion torque during the swing phase and dorsiflexion motion control in the initial contact phase. By using the OpenSim 2392 model, dorsiflexor muscle activity is achieved for normal gait. As shown in Fig. 6, the tibialis anterior and digitorum longus muscles are more active than the extensor and peroneus tertius muscles in the swing and initial contact phase. Hence, in drop foot patients, tibialis anterior and digitorum longus muscle weakness is more pronounced in patients with motor disability. In this study, the swing and loading response phase, as shown with the gray area in Fig. 6, includes 5-50% of the gait cycle based on the patient's ankle joint kinematic.

The aforementioned algorithm for designing a patient-specific AFO for drop foot patients using SMA is shown in Fig. 7.

7. Results and discussion

Most researchers in previous studies have assumed that the patient with drop foot cannot perform dorsiflexion; therefore, they provided all the dorsiflexion torque required for a healthy ankle joint during the swing and initial contact phases to reproduce the stiffness of a normal ankle. Many patients with moderate muscle weakness can use the dorsiflexion torque during the gait cycle, and the creation of a total dorsiflexion torque does not require a healthy ankle. Applying unnecessary pressure on the calf muscles and muscle weakness in the remaining healthy pretibial fibers can lead to this hypothesis.

As mentioned above, the pretibial area consists of four muscles: tibialis anterior, extensor, digitorum longus and peroneus tertius, and patients with various levels of pretibial deficiency have a disability in one or more of these muscles. As a result, the level of muscle deficiency varies among the different scenarios, and the torque curve of the actuator is also expected to vary. The required torque to correct the kinematics of each scenario should be calculated individually. In this study, 15 scenarios with various levels of pretibial deficiency in one or more of the aforementioned muscles were simulated in OpenSim. The ankle actuator torque in a simulation with a different amount of weakness in the pretibial muscles needs the same amount of correction for gait pattern in the following scenarios. Tables 4 and 5 show different scenarios that require the same amount of torque for the first and third patients to correct their gait pattern. Consequently, designing the passive orthosis to correct the gait pattern for the first and third patients includes all these scenarios.

Table 5
Characteristic of scenarios with similar levels of pretibial muscles weakness to the third patient.

Scenarios	Tibialis anterior	Extensor	Digitorum longus	Peroneus tertius
Fourth scenario	+	–	–	–
Fifth scenario	–	–	+	+
Sixth scenario	+	+	–	–

The orthosis in this study was designed for three patients with different levels of pretibial muscles weakness and the same procedure was shown to be suitable for any patient with pretibial weakness. Patients with muscle weakness who cannot generate dorsiflexion torque are aided by the SMA element, which is embedded in the proposed orthosis. This study also showed that a linear torsional spring can be used to reproduce ankle joint stiffness. As shown in Fig. 8, the stiffness of the linear torsional spring that is embedded to regenerate ankle joint stiffness in the patients was $105\,kg\,m^2\,s^{-2}$, $75\,kg\,m^2\,s^{-2}$ and $60\,kg\,m^2\,s^{-2}$ for the first, second and third patients, respectively. Although linear torsional spring stiffness may be more compatible with the actuator (simulated) stiffness, orthosis with a linear torsional spring has several disadvantages: heaviness and bulkiness of the

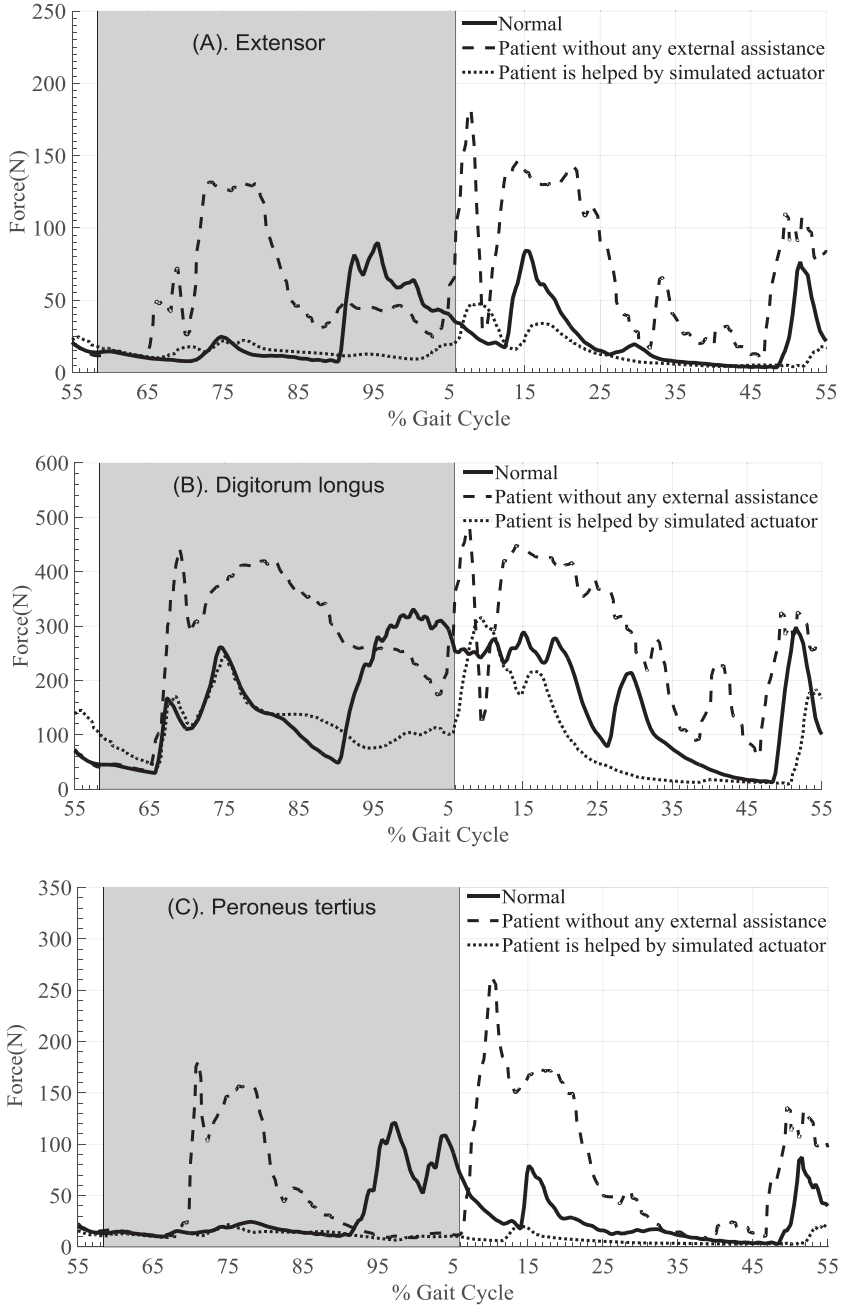

Fig. 10. The gait cycle for three cases: a healthy subject, the third patient with muscle weakness, and when using the actuator.

mechanism; the need for an alloy that does not show plastic deformity under the existing loading; and the undesirable linear mechanical properties of the linear torsional spring, which lead to damping the ground reaction force in the initial contact phase. The SMA element was utilized in the proposed orthosis because it is compatible with the human body, has desirable non-linear mechanical properties, hysteresis characteristics, low volume and reduced weight.

Fig. 8 shows the torque produced by manipulating the cross-section of the SMA element and by changing the stiffness of the linear torsional spring to reproduce the ankle joint stiffness in patients with different levels of muscle weakness. The intersection dimensions of the SMA element were $17 \times 10\,mm^2$, $15 \times 9\,mm^2$ and $13 \times 9\,mm^2$ for the first, second and third patients, respectively. In all cases, the shape of the SMA or linear spring was considered to be 270°, as shown in Fig. 3. The width of the SMA beam should be sufficient to reproduce the stiffness of the actuator. However, there is a maximum beam width to ensure patients do not encounter any problems while using the device under their clothing. Both demands are met by a maximum width of 17 mm.

In terms of muscle activity, the peroneus tertius muscle in the second patient and the extensor and peroneus tertius muscles in the third patient were healthy. For the second and third patients, muscular activity during the gait cycle is shown in Figs. 9 and 10, respectively, where the curves include that of a healthy person and a patient suffering muscle weakness with and without the proposed orthosis. These muscles have normal activity in a healthy person. However, when other dorsiflexor muscles are weak, the rest of the healthy muscles compensate for the weakness by generating more torque. Enhancing the activity of these muscles slightly improves the patient's kinematics, but cannot compensate for the weakness of the other extensor muscles. The excessive activity of the rest of the healthy muscles leads to insecure gait cycles and causes fatigue and damage to the muscles. In cases where the patient uses orthosis in all three of these muscles, the activity of these muscles returns to the normal level and prevents possible damages in the swing and loading response phase, which starts in 5–50% of gait cycles in Fig. 9 (A and B).

8. Summary and conclusion

A few orthoses can help dorsiflexion movement during the gait cycle. However, these devices cannot be used daily because of their large volume and weight, the need for an external power supply, and the high costs associated with the complex control system. Furthermore, conventional passive devices do not provide a patient-specific stiffness profile intended for each type of deficiency. In this paper, an orthosis was designed to imitate the stiffness of a healthy ankle joint. Adding the SMA element on the hinged AFO to stimulate dorsiflexion reduces toe drag. Similarly, the SMA element can be used to apply force towards dorsiflexion in the stance phase, in which controlled plantar flexion will prevent slap foot. The device presented in this study was designed specifically for three patients with different levels of pretibial muscle weakness; the study illustrated that this process can be used for all patients with pretibial weakness. Motion analysis tests were used for each patient to optimize the torque needed to correct the kinematics according to muscle stimulation and activity during the gait cycle. OpenSim was utilized to simulate patients with muscle weakness and to calculate the torque required to imitate normal ankle joint stiffness. The normal joint stiffness profile for each patient with a certain level of muscle weakness can be restored by designing a patient-specific orthosis. Dimensions of the SMA element were calculated by simulating it in ABAQUS to generate the torque required for the patient during the swing and initial contact phases.

Conflicts of interest

The authors declared no potential conflicts of interest with respect to the research, authorship, and/or publication of this article.

Funding

This study was funded by the corresponding author.

Ethical approval

Not required.

References

[1] Kirkup JR. A history of limb amputation. Springer Science & Business Media; 2007.
[2] Seel T, Werner C, Schauer T. The adaptive drop foot stimulator–multivariable learning control of foot pitch and roll motion in paretic gait. Med Eng Phys 2016;38(11):1205–13.
[3] NINDS Foot Drop Information Page. National Institute of Neurological Disorders and Stroke. National Institutes of Health, 2009.
[4] Simonsen EB, Moesby LM, Hansen LD, Comins J, Alkjaer T. Redistribution of joint moments during walking in patients with drop-foot. Clin Biomech 2010;25(9):949–52.
[5] Gracies JM. Pathophysiology of spastic paresis. I: paresis and soft tissue changes. Muscle Nerve 2005;31(5):535–51.
[6] Gracies JM. Pathophysiology of spastic paresis. II: emergence of muscle overactivity. Muscle Nerve 2005;31(5):552–71.
[7] Bregman DJ, De Groot V, Van Diggele P, Meulman H, Houdijk H, Harlaar J. Polypropylene ankle foot orthoses to overcome drop-foot gait in central neurological patients: a mechanical and functional evaluation. Prosthet Orthot Int 2010;34(3):293–304.
[8] Nielsen CC. Issues affecting the future demand for orthotists and prosthetists: update 2002: a study updated for the national commission on orthotic and prosthetic education. National Commission on Orthotic and Prosthetic Education; May 2002. 2002.
[9] Wu KK. Foot orthoses: principles and clinical applications, 26. Williams & Wilkins; 1990.
[10] Kobayashi T, Orendurff MS, Hunt G, Lincoln LS, Gao F, LeCursi N, et al. An articulated ankle-foot orthosis with adjustable plantarflexion resistance, dorsiflexion resistance and alignment: a pilot study on mechanical properties and effects on stroke hemiparetic gait. Med Eng Phys 2017;44:94–101.
[11] Bhadane-Deshpande M. Towards a shape memory alloy based variable stiffness ankle foot orthosis. The University of Toledo; 2012.
[12] Deberg L. A fast actuator using shape memory alloys for an ankle foot orthosis Master's thesis. Ecole Supérieure des Sciences et Technologies de l'Ingénieur de Nancy; 2012.
[13] Deberg L, Andani MT, Hosseinipour M, Elahinia M. An SMA passive ankle foot orthosis: design, modeling, and experimental evaluation. Smart Mater Res 2014 Article ID 57209411. doi:10.1155/2014/572094.
[14] Andani MT, Elahinia M. Modeling and simulation of SMA medical devices undergoing complex thermo-mechanical loadings. J Mater Eng Perform 2014;23(7):2574–83.
[15] Mataee MG, Andani MT, Elahinia M. Adaptive ankle-foot orthoses based on superelasticity of shape memory alloys. J Intell Mater Syst Struct 2015;26(6):639–51.
[16] Pittaccio S, Viscuso S, Beretta E, Turconi AC, Strazzer S. Pilot studies suggesting new applications of NiTi in dynamic orthoses for the ankle joint. Prosthet Orthot Int 2010;34(3):305–18.
[17] Facchinello Y, Brailovski V, Petit Y, Mac-Thiong JM. Monolithic superelastic rods with variable flexural stiffness for spinal fusion: modeling of the processing-properties relationship. Med Eng Phys 2014;36(11):1455–63.
[18] Rueterbories J, Spaich EG, Larsen B, Andersen OK. Methods for gait event detection and analysis in ambulatory systems. Med Eng Phys 2010;32(6):545–52.
[19] Poorasadion S, Arghavani J, Naghdabadi R. An improvement on the Brinson model for shape memory alloys with application to two-dimensional beam element. J Intell Mater Syst Struct 2014;25(15):1905–20.
[20] Gage J. An overview of normal walking. Instr Course Lect 1990;39:291.
[21] Perry J, Davids JR. Gait analysis: normal and pathological function. J Pediatr Orthop 1992;12(6):815.
[22] Davis RB, DeLuca PA. Gait characterization via dynamic joint stiffness. Gait Posture 1996;4(3):224–31.
[23] Capaday C. The special nature of human walking and its neural control. Trends Neurosci 2002;25(7):370–6.
[24] Ludvig D, Kearney RE. Intrinsic, reflex and voluntary contributions to task-dependent joint stiffness. In: Proceedings of the annual international conference of the IEEE engineering in medicine and biology society (EMBC). IEEE; 2010.
[25] Mirbagheri M, Kearney R, Barbeau H. Intrinsic and reflex contributions to human ankle stiffness: variation with ankle position. In: Proceedings of the eleventh conference of the international society of electrophysiology and kinesiology; 1996.

[26] McHugh B. Analysis of body-device interface forces in the sagittal plane for patients wearing ankle-foot orthoses. Prosthet Orthot Int 1999;23(1):75–81.
[27] Hansen AH, Childress DS, Miff SC, Gard SA, Mesplay KP. The human ankle during walking: implications for design of biomimetic ankle prostheses. J Biomech 2004;37(10):1467–74.
[28] Lelas JL, Merriman GJ, Riley PO, Kerrigan DC. Predicting peak kinematic and kinetic parameters from gait speed. Gait Posture 2003;17(2):106–12.
[29] Pittaccio S, Garavaglia L, Ceriotti C, Passaretti F. Applications of shape memory alloys for neurology and neuromuscular rehabilitation. J Funct Biomater 2015;6(2):328–44.
[30] Lagoudas DC. Shape memory alloys: modeling and engineering applications. Springer Science & Business Media; 2008.
[31] Brinson L, Huang M. Simplifications and comparisons of shape memory alloy constitutive models. J Intell Mater Syst Struct 1996;7(1):108–14.
[32] Sayyaadi H, Zakerzadeh MR, Salehi H. A comparative analysis of some one-dimensional shape memory alloy constitutive models based on experimental tests. Sci Iran 2012;19(2):249–57.
[33] Tokuda M, Ye M, Takakura M, Sittner P. Thermomechanical behavior of shape memory alloy under complex loading conditions. Int J Plast 1999;15(2):223–39.
[34] Thelen DG, Anderson FC. Using computed muscle control to generate forward dynamic simulations of human walking from experimental data. J Biomech 2006;39(6):1107–15.